MMCFormer: Missing Modality Compensation Transformer for Brain Tumor Segmentation

Author name(s) withheld EMAIL(S) WITHHELD
Address withheld

Editors: Under Review for MIDL 2023

Abstract

Human brain tumours and more specifically gliomas are amongst the most life-threatening cancers which usually arise from abnormal growth of the glial stem cells. In practice, Magnetic Resonance Imaging (MRI) modalities, which offer different contrasts to elucidate tissue properties, provide comprehensive information regarding the brain's structure and also potential clues for detecting tumors. Hence, multi-modal MRI is commonly utilized for the diagnosis of brain tumors. However, since the set of acquired modalities may vary between clinical sites, brain tumor studies may miss one or two MRI modalities. To address missing information in an end-to-end manner, we propose MMCFormer, a novel missing modality compensation network. Our strategy builds upon 3D efficient transformer blocks and uses a co-training strategy to effectively train a missing modality network. To ensure feature consistency in a multi-scale fashion, MMCFormer utilizes global contextual agreement modules in each scale of the encoders. Furthermore, to transfer modality-specific representations, we propose to incorporate auxiliary tokens in the bottleneck stage to model interaction between full and missing-modality paths. On top of that, we include feature consistency losses to reduce the domain gap in network prediction and increase the prediction reliability for the missing modality path. Extensive experiments on the BraTS 2018 dataset demonstrate the benefits of our approach compared to competing approaches. The implementation code will be publicly available after the paper acceptance.

Keywords: Transformer, Missing Modality, Segmentation, MRI, Medical.

1. Introduction

Magnetic Resonance Imaging (MRI) is a prevalent non-invasive imaging utility commonly used in medical diagnosis and treatment that can provide a 3D representation of human organs, tissues, and the skeletal system. However, interpretation of the data by a clinical expert (e.g. localizing and segmenting the brain tumor) is typically time-consuming and expensive. In addition, due to inter- and intra-rater variabilities, clinical expert annotations are always accompanied by uncertainties. Therefore, multi-modal MRI imaging (e.g. T1, T1c, T2, and Flair modalities) can be beneficial since it aggregates complementary modality-specific information and allows more accurate pathology assessment. However, acquiring all desirable imaging modalities sometimes is not feasible due to practical constraints, such as lengthy scan time and image corruption. Hence, a missing modality issue may raise uncertainty for tumour localization and segmentation, since each modality contributes unique and comprehensive information (Azad et al., 2022b; Zhao et al., 2022).

Several methods have been presented to solve the problem of automatic segmentation. Over the past decade, Convolutional Neural Networks (CNNs) have been instrumental in

© 2023 Anonymous.

the development of medical image segmentation, such as UNet (Ronneberger et al., 2015), and its variants (Valanarasu et al., 2020; Zhou et al., 2018; Azad et al., 2022a), which have been widely used due to their symmetric architecture and potentiality to capture contextual semantic information while preserving multi-scale features with skip connections. Recently, the introduction of the Vision Transformer (ViT) has substantially improved the performance of all computer vision tasks by including an attention mechanism that effectively captures global information (Dosovitskiy et al., 2020). Since then, Transformers have been diligently deployed in medical image segmentation to compensate for CNNs' inability to capture sufficient contextual information, yielding poor performance in boundary areas. Motivated by the U-shaped architecture of UNet, Swin-UNet (Cao et al., 2021), and DS-TransUNet (Lin et al., 2022) propose pure transformer models based on Swin Transformer for image segmentation. Similarly, MISSFormer (Huang et al., 2021) employs a hierarchical symmetric encoder-decoder Transformer coupled with the enhanced Transformer block to boost the feature representations. Aside from fully-Transformer models, various approaches have been presented that employ both CNNs and Transformers together to acquire low-level and high-level features (Heidari et al., 2022; Chen et al., 2021). However, these models require the presence of all modalities to provide their excellent results. Otherwise, in case of a missing modality, their performance would decrease.

Several methods have been proposed for dealing with missing data in medical imaging. Early approaches aim at synthesizing the missing modality during the training process (Azad et al., 2022b). However, reconstructing the missing modality usually requires designing a modality-specific network and limits the performance of these strategies for end-to-end training. Therefore, more recent methods adopt a more efficient strategy, building a uniform model for all possible missing modalities by learning full modality joint representations. HEMIS (Havaei et al., 2016) proposes to encode each modality into an embedding space using separate convolutional layers. Afterward, the embedded features' first and second-order moments (mean and variance) are calculated to establish a common representation space between modalities. During inference, any combination of inputs can be given to construct the segmentation map. The same strategy is followed by PIMMS (Varsavsky et al., 2018), HVED (Dorent et al., 2019), and URN (Lau et al., 2019) in creating a common latent subspace and seeking to retrieve the missing information using the constructed latent representation. However, such approaches are unable to provide adequate information using only mean and variance and yield poor performance when more than one modality is absent.

In recent years, Generative Adversarial Networks (GANs) have been established for generating synthetic data (Qin et al., 2022; Chang et al., 2020; Cao et al., 2020; Sharma and Hamarneh, 2019). Nevertheless, employing GAN-based models to tackle the missing modality problem raises several difficulties. In addition to possibly generating undesirable imputation noise when synthesizing the missing modality, they can also show non-converging characteristics, require extensive and careful training, and the generator is likely to become unstable during training.

Other approaches, such as the networks described by (Azad et al., 2022c; Liu et al., 2022; Wang et al., 2021), take advantage of the knowledge distillation strategy. They offer a co-training strategy for training the "complete modality" and "missing modality" models simultaneously in order to complement each other's feature representations and restore missing knowledge of missing modalities. However, their models rely on the CNN

structure and are therefore unable to effectively capture structural and shape information (e.g., learning brain structure and detecting abnormal regions) from the "full modality" path, resulting in less accurate prediction when facing several missing modalities. Besides that, these methods only perform feature recalibration between the "full modality" and the "missing modality" paths and lack to imitate the modality-specific information and contextual consistency. In this paper, we argue that contextual consistency is crucial for the segmentation task and seek to model such consistency with the Transformer model. Furthermore, we propose to modify the bottleneck representation by including additional tokens to learn modality-specific representation and compensate for the missing information. We create our architecture in a pure Transformer fashion with efficient self-attention blocks and perform the co-training strategy in an end-to-end manner.

2. Proposed Method

The overall structure of the proposed MMCFormer is depicted in Figure 1. MMCFormer is a novel pure Transformer-based approach that adopts the co-training strategy for the MRI missing modality task, where one network is assigned to train the complete modality while the other trains with the missing modality. Co-training is a multi-view algorithm that predicts every data point from two independent views (Rahate et al., 2022). These two views are trained independently and complement one another since both provide unique, complementary information. On the other hand, MRI modalities have shown that they can provide comprehensive and distinguishable features of brain structure that enable physicians to have more accurate anatomical and functional examinations. To this end, taking an input 3D modality image $X_i \in R^{H\times W\times D\times C}$ with spatial dimensions $H \times W \times D$ and C channels (i.e. modalities), we can describe the full-modality data as $X_f = \{\forall X_i, i \in M\}$, and the missing modality as $X_m = \left\{\forall X_i, i \in M^{'}\right\}$, where M indicates the set of modalities (T1, T1w, T2 and Flair) and $M^{'}$ can be any subset of M (i.e., $M^{'} \subset M$). We define two parallel 3D efficient Transformers U-Net models for our co-training strategy, where each network is trained separately and simultaneously. One is trained on the complete data (X_f) to obtain comprehensive information about the full modality, and the second one is trained on the incomplete data (X_m) to derive the missing modalities details. The co-training strategy allows the "full modality" network to distill its knowledge into the "missing modality" one, and compensate for the lack of modality-specific information. In the next subsections, we first present our network structure and then present our knowledge distillation mechanisms.

2.1. Network Architecture

As stated earlier, our network builds upon an efficient Transformer design to reduce the computational burden of 3D data processing. More precisely, for an input image $X^{H\times W\times D\times C}$, we first perform the tokenization process by extracting n non-overlapping 3D patches and applying the parametric mapping function to embed each token into a d dimensional space. Next, following the general idea of the self-attention mechanism, we create the Q, K, and V matrices using linear projections. However, instead of applying the basic self-attention module, which suffers from a quadratic computational complexity, we follow the efficient self-attention strategy (Shen et al., 2021)

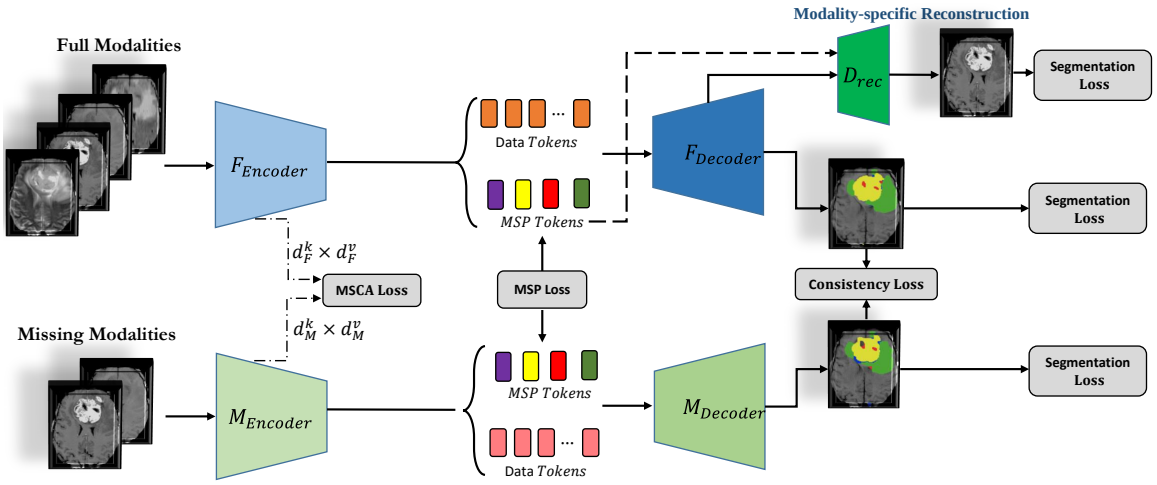

Figure 1: Overview of the proposed MMCFormer. MMCFormer deploys three feature-matching mechanisms to reduce the domain gap and to ensure knowledge distillation from the "full modality" path into a "missing modality" network.

$$E(Q, K, V) = \rho_q(Q)\left(\rho_k(k)^T V\right), \tag{1}$$

where ρ shows the softmax operation. It was shown that (Shen et al., 2021) the efficient self-attention module can approximate the standard self-attention operation but with much lower computational complexity, $O(d^2 n)$ vs $O(n^2)$ (Shen et al., 2021). Where d and n indicate the embedding dimension and the number of tokens, respectively. For our U-Net structure, we follow a symmetrical design and include three efficient Transformer blocks in each encoder/decoder block. We use patch merging and patch expanding layers in the encoding and decoding paths, respectively. Finally, we include the skip-connection path in each scale of the network to capture multi-scale representations. The same structure is used in both the "full modality" and the "missing modality" network. For training, two main and three auxiliary loss functions are applied to reconstruct the segmentation map and ensure the knowledge distillation between the full modality and the missing modality paths. Our first primary loss function is the Dice loss, which computes the loss between the ground truth Y and the predicted mask $Y^{'}$ to learn the segmentation map:

$$\mathcal{L}_{\text{seg}} = \alpha \mathcal{L}_{\text{dice}}\left(Y_f', Y\right) + \beta \mathcal{L}_{\text{dice}}\left(Y_m', Y\right) \tag{2}$$

In the training step, we set α to 0.6, and β to 0.4. In the second step, we follow (Azad et al., 2022c) and design a consistency loss function to reduce the domain gap between the "full modality" and the missing one, aiming to reduce the distance between the two distributions and increase the confidence of the "missing modality" model. Thus, our approach will improve the boundary area estimation in cases where the uncertainty (or entropy) of pixels is high or when the probability of a pixel belonging to a class is low. Equation 3 illustrates our consistency loss function:

$$\mathcal{L}_{Consistency}\left(S_f, S_m\right) = \sum_{i=1}^{c} \left|S_f^i - S_m^i\right| \tag{3}$$

where, S^i indicates the soft prediction map in the i_{th} channel of the network in each path. Next, we design and employ two knowledge distillation modules, namely Multi-Scale Contextual Agreement (MSCA) and Modality-Specific (MSP) tokens, to ensure the effective distillation of the semantic and contextual information associated with the full-modality model into the missing one, as outlined in the next subsection.

2.2. Knowledge Distillation Modules

Multi-Scale Contextual Agreement (MSCA) Module: Considering a rich representation of the full-modality path, we aim to impose a hierarchical knowledge distillation module to the missing-modality path to adaptively recalibrate its feature representation and minimize the domain gap. To this end, we propose the MSCA module, which seeks to minimize the context distribution between the missing and full-modality paths in each scale of the network. In our efficient self-attention mechanism, we compute the global context (GC) using the query and value vectors as $GC = (\rho_k(k)^T V) \in R^{d\times d}$. To effectively align the correlation matrix calculated in both paths (GC_f and GC_m), we strive to minimize the distance as follows:

$$\mathcal{L}_{\text{MSCA}}\left(\mathbf{GC}_f, \mathbf{GC}_2\right) = 1 - \frac{\operatorname{tr}\left\{\mathbf{GC}_f \mathbf{GC}_m\right\}}{\|\mathbf{GC}\| \, \|\mathbf{GC}_m\|} \quad \in [0,1] \tag{4}$$

The $\mathcal{L}_{\text{MSCA}}$ becomes zero when the correlation matrices are equal and one if they have maximum difference. Using the inner product, the above equation can be reformulated as:

$$\mathcal{L}_{\text{MSCA}}\left(\mathbf{GC}_f, \mathbf{GC}_m\right) = 1 - \frac{\left\langle \operatorname{vec}\left\{\mathbf{GC}_f\right\}, \operatorname{vec}\left\{\mathbf{GC}_m\right\}\right\rangle}{\|\operatorname{vec}\left\{\mathbf{GC_f}\right\}\|_2 \, \|\operatorname{vec}\left\{\mathbf{GC_m}\right\}\|_2} \tag{5}$$

The reformulated equation calculates the orthogonality among correlation matrices in $d \times d$ dimensional space. To make this more clear, the product between the correlation matrices can be written by means of the eigenvalue decomposition:

$$\mathbf{GC}_f \mathbf{GC}_m = \mathbf{U}_1 \mathbf{\Lambda}_1 \mathbf{U}_1^H \mathbf{U}_2 \mathbf{\Lambda}_2 \mathbf{U}_2^H = \mathbf{U}_1 \mathbf{D} \mathbf{U}_2^H \tag{6}$$

$$(\mathbf{D})_{ij} = \mathbf{u}_{(1),i}^H \mathbf{u}_{(2),j} \lambda_{(1),i} \lambda_{(2),j} \tag{7}$$

where D_{ij} represents the entry at position (i, j) of D. Also, $u_{(1),i}$ and $u_{(2),j}$ are the ith and jth column of U_1 and U_2, respectively and $\lambda_{(1),i}$ and $\lambda_{(2),j}$ show the corresponding eigenvalue. The value of D becomes zero if $u_{(1),i}$ and $u_{(2),j}$ are orthogonal or either $\lambda_{(1),i}$ or $\lambda_{(2),j}$ is zero. The zero matrix for D results in $tr(GC_f GC_m)$ being zero, and as a result, the correlation matrix becomes one. However, more overlap in the signal spaces of GC_f and GC_m brings a higher effect in the product and a decrease in $\mathcal{L}_{MSCA}$. Thus, the design of $\mathcal{L}_{MSCA}$ is well suited to align the correlation of the "missing modality" path with the "full-modality" one.

Modality Specific (MSP) Module: In the MSCA module, we aimed to align the feature distribution between the two networks. However, such alignment might suppress the discriminative modality-specific (MS) features that existed in the full-modality paths. Therefore, we design the MSP module to preserve discriminative features in the full path and transfer this information to the missing-modality path. For this purpose, we define four

modality-specific tokens in the network bottleneck, where each token aims to preserve distinctive features of each input modality. We choose bottleneck since it contains highly condensed low-dimensional information of label maps, hence, we can exploit its useful and distinctive features to distill the modality-specific knowledge to the "missing modality" network. Thus, MSP loss is calculated using the output of full and missing tokens from the bottleneck, culminating in transferring modality-specific distinguishing features from the complete model to the incomplete one. The MSP loss is defined as:

$$\mathcal{L}_{MSP}\left(MSP_f, MSP_m\right) = \sum_{i=1}^{M} |MSP_f^i - MSP_m^i| \tag{8}$$

This soft-aligned feature representation helps the missing-modality path to reconstruct the discriminative features which are not feasible through its incomplete input modalities. We finally devise a reconstruction loss in the full-modality path to ensure that each token learns modality-specific information. To do so, we employ an auxiliary reconstruction decoder head (D_{rec}) alongside the segmentation head to perform the reconstruction task. In each step, we randomly take one of the tokens alongside the resultant feature maps from the previous decoder layer to input into the reconstruction decoder, seeking to reconstruct the modality assigned to the class token. By doing so, we can guarantee that each token learns distinctive modality information. For the reconstruction loss, we use the combination of MS-SSIM and L1 distance (Zhao et al., 2016) to better reconstruct the high-frequency information alongside the image content, which are crucial for the MRI modalities:

$$\mathcal{L}_{recon} = \theta \underbrace{\left[1 - l_M(\tilde{p}) \cdot \prod_{j=1}^{M} cs_j(\tilde{p})\right]}_{\mathcal{L}_{\text{MS-SSIM}}} + (1-\theta).G_{\sigma_G^M} . \underbrace{\frac{1}{N} \sum_{p \in P} |X_i(p) - Y_{recon}^{'}(p)|}_{\mathcal{L}_{\ell_1}} \tag{9}$$

where $Y_{recon}^{'}$ is the reconstruction output. l_M and cs_j are derived from SSIM Equation 10 at scales M and j.

$$\text{SSIM}(p) = \frac{2\mu_x\mu_y + C_1}{\mu_x^2 + \mu_y^2 + C_1} \cdot \frac{2\sigma_{xy} + C_2}{\sigma_x^2 + \sigma_y^2 + C_2} = l(p) \cdot cs(p) \tag{10}$$

p stands for pixel. According to (Zhao et al., 2016), means and standard deviations are calculated using a Gaussian filter with a standard deviation σ_G, denoted G_{σ_G}. Moreover, MS-SSIM, a multi-scale form of SSIM, necessitates observing pixels at a neighbourhood of p within a window with the same kernel size as G_{σ_G}, whereas calculating its derivative is infeasible in some boundary regions. Hence, the loss for the whole window is approximated by computing loss at its center pixel $\tilde{p}$.

2.3. Joint Objective

Eventually, the overall loss function $\mathcal{L}$ is formulated by:

$$\mathcal{L} = \mathcal{L}_{seg} + \lambda_0\mathcal{L}_{con} + \lambda_1\mathcal{L}_{MSCA} + \lambda_2\mathcal{L}_{MSP} + \lambda_3\mathcal{L}_{recon} \tag{11}$$

To determine the contribution of each loss to the overall loss value, we use λ coefficients, which are set experimentally. The model is trained using Adam optimization with a learning rate of $1e-4$ and batch size 1 for 200 epochs. In addition, the code is developed in PyTorch, and the model is trained on a single RTX 3090 GPU.

3. Experimental Results

3.1. Dataset and Evaluation Metric

For performance evaluation, we use the BraTS 2018 dataset (Menze et al., 2014; Bakas et al., 2018), which is commonly used for benchmarking brain glioma segmentation pipelines with well-curated multi-institutional MRI data. This dataset includes 250 cases, each with four 3D MRI modalities (T1, T1c, T2, and FLAIR) rigidly aligned, resampled to $1 \times 1 \times 1$ mm isotropic resolution, and skull-stripped. The input volumetric spatial data size is 240×240 with 155 slices each. Annotations for the BraTS dataset include three tumor subregion classes: the enhancing tumor, the peritumoral edema, and the necrotic and non-enhancing tumor core. In our experiment, we follow the pre-processing steps and the same input size ($160 \times 192 \times 128$) as suggested in (Azad et al., 2022c) to evaluate our network in terms of the Dice Similarity Coefficient (DSC).

3.2. Comparative Results

In Table 1, we provide the comparative results on each combination of the missing modality scenario. In comparison to the HeMIS(Havaei et al., 2016) and HVED (Dorent et al., 2019) strategies, our approach produces better segmentation results, specifically in the single modality (e.g., only T2) scenario. Moreover, SMU-Net (Azad et al., 2022c) proposes to decompose the representational space into style and content vectors and then strives to minimize the distribution difference between the full and missing modality path to perform knowledge distillation. Similarly, the ACN (Wang et al., 2021) takes the same perspective and performs the knowledge distillation in terms of both style and content modules but without separating them. Although both approaches strive to maximize the similarity between full and missing networks, they lack to include a mechanism to preserve the modality-specific features and distill such representation to the "missing modality" network. On the contrary, our approach proposes MSP tokens combined with the reconstruction head to guarantee such information preservation and performance gain. Quantitatively, compared to HeMIS and HVED, our approach significantly improves the performance by a 12-49 Dice score for single modality scenarios. In addition, compared to SMU-Net and the ACN approaches, the DSC score slightly rises by 0.5-2 Dice score. Visual segmentation results are presented in Figure 2 for single modality scenarios. It can be observed that the model can predict the brain tumour regions, whereas such prediction was not feasible by only relying on the input data without reconstructing the missing information.

Table 1: Performance comparison on the BraTS 2018 dataset using Dice metric. HeM, HVE, and MMC indicate the HeMIS, HVED, and our proposed MMCFormer models, respectively.

Modalities				Complete					Core					Enhancing				
Flair	T1	T1c	T2	HeM	HVE	ACN	SMU	MMC	HeM	HVE	ACN	SMU	MMC	HeM	HVE	ACN	SMU	MMC
○	○	○	●	79.2	80.9	85.4	**85.7**	84.1	50.5	54.1	66.8	67.2	**69.7**	23.3	30.8	41.7	43.1	**50.7**
○	○	●	○	58.5	62.4	79.8	80.3	**80.4**	58.5	66.7	83.3	84.1	**86.6**	60.8	65.5	78.0	78.3	**79.0**
○	●	○	○	54.3	52.4	78.7	**78.6**	78.6	37.9	37.2	**70.9**	69.5	69.3	12.4	13.7	41.8	42.8	**42.9**
●	○	○	○	79.9	82.1	87.3	**87.5**	86.2	49.8	50.4	66.4	**71.8**	70.0	24.9	24.8	42.2	46.1	**49.6**
○	○	●	●	81.0	82.7	84.9	86.1	**86.3**	69.1	73.7	83.2	85.0	**86.7**	68.6	70.2	74.9	75.7	**79.1**
○	●	●	○	63.8	66.8	79.6	**80.3**	80.2	64.0	69.7	83.9	84.4	**86.6**	65.3	67.0	75.3	75.1	**78.7**
●	●	○	○	83.9	84.3	86.0	87.3	**87.7**	56.7	55.3	70.4	71.2	**72.0**	29.0	24.2	42.5	44.0	**48.1**
○	●	○	●	80.8	82.2	84.4	85.6	**85.9**	53.4	57.2	72.8	73.5	**74.0**	28.3	30.7	46.5	**47.7**	46.9
●	○	○	●	86.0	87.5	86.9	87.9	**88.0**	58.7	59.7	70.7	71.2	**72.4**	28.0	34.6	44.3	46.0	**48.3**
●	○	●	○	83.3	85.5	87.8	88.4	**88.7**	67.6	72.9	82.9	84.1	**86.7**	68.0	70.3	77.5	77.3	**79.5**
●	●	●	○	85.1	86.2	**88.4**	88.2	88.3	70.7	74.2	83.3	84.2	**86.6**	69.9	71.1	75.1	76.2	**78.1**
●	●	○	●	87.0	88.0	87.4	88.3	**88.5**	61.0	61.5	67.7	**67.9**	67.8	33.4	34.1	42.8	43.1	**50.7**
●	○	●	●	87.0	88.6	87.2	88.2	**88.9**	72.2	75.6	82.9	82.5	**86.6**	69.7	71.2	73.8	75.4	**79.1**
○	●	●	●	82.1	83.3	86.6	86.5	**86.8**	70.7	75.3	83.2	84.4	**86.7**	69.7	71.1	75.9	76.2	**79.2**
●	●	●	●	87.6	88.8	89.1	88.9	**89.0**	73.4	76.4	84.8	87.3	**87.4**	70.8	71.7	78.2	79.3	**80.1**
Mean				78.6	80.1	85.3	**85.9**	**85.9**	59.7	64.0	76.8	77.9	**79.2**	48.1	50.1	60.70	61.8	**64.7**

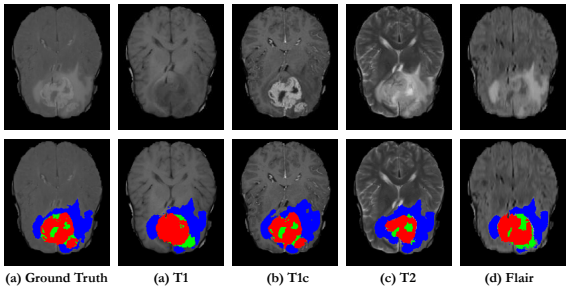

(a) Ground Truth (a) T1 (b) T1c (c) T2 (d) Flair

Figure 2: Segmentation results of the MMCFormer in single modality setting using BraTS 2018 dataset. The WT, edema, and necrotic regions are visualized with blue, red, and green colors.

Table 2: Contribution of each MMCFormer module on the overall performance. For all experiments, only the T2 modality was used as input for the missing modality network.

$\mathcal{L}_{\text{MCA}}$	$\mathcal{L}_{\text{MSP}}$	$\mathcal{L}_{\text{recon}}$	WT	CT	ET	Average
✗	✓	✓	83.7	69.2	49.7	67.6
✓	✗	✓	82.1	66.6	47.9	65.6
✓	✓	✗	84.0	68.9	50.3	67.7
✓	✓	✓	84.1	69.7	50.7	68.2

3.3. Ablation Study

To analyze the effect of each module on the overall performance, we also provide an ablation study in Table 2. It can be observed that by eliminating each module from the proposed structure, the overall performance slightly decreases. The largest performance drop happens when the MSP tokens are eliminated, hence, showing the importance of preserving MS features. Further ablation studies are provided in the Appendix section.

4. Conclusion

To address missing modality correction in an end-to-end manner, we proposed our MMCFormer model, which utilizes a co-training strategy to perform knowledge distillation from the full-modality network into a missing modality one. To preserve modality-specific features, we proposed MSP tokens in conjunction with the reconstruction head to distill more discriminative features to the "missing modality" network. We also included a context agreement module to refine the feature representation in each scale of the co-training strategy.

References

Reza Azad, Ehsan Khodapanah Aghdam, Amelie Rauland, Yiwei Jia, Atlas Haddadi Aval, Afshin Bozorgpour, Sanaz Karimijafarbigloo, Joseph Paul Cohen, Ehsan Adeli, and

Dorit Merhof. Medical image segmentation review: The success of u-net. *arXiv preprint arXiv:2211.14830*, 2022a.

Reza Azad, Nika Khosravi, Mohammad Dehghanmanshadi, Julien Cohen-Adad, and Dorit Merhof. Medical image segmentation on mri images with missing modalities: A review. *arXiv preprint arXiv:2203.06217*, 2022b.

Reza Azad, Nika Khosravi, and Dorit Merhof. Smu-net: Style matching u-net for brain tumor segmentation with missing modalities. *arXiv preprint arXiv:2204.02961*, 2022c.

Spyridon Bakas, Mauricio Reyes, Andras Jakab, Stefan Bauer, Markus Rempfler, Alessandro Crimi, Russell Takeshi Shinohara, Christoph Berger, Sung Min Ha, Martin Rozycki, et al. Identifying the best machine learning algorithms for brain tumor segmentation, progression assessment, and overall survival prediction in the brats challenge. *arXiv preprint arXiv:1811.02629*, 2018.

Bing Cao, Han Zhang, Nannan Wang, Xinbo Gao, and Dinggang Shen. Auto-gan: self-supervised collaborative learning for medical image synthesis. In *Proceedings of the AAAI conference on artificial intelligence*, volume 34, pages 10486–10493, 2020.

Hu Cao, Yueyue Wang, Joy Chen, Dongsheng Jiang, Xiaopeng Zhang, Qi Tian, and Manning Wang. Swin-unet: Unet-like pure transformer for medical image segmentation. *arXiv preprint arXiv:2105.05537*, 2021.

Qi Chang, Zhennan Yan, Lohendran Baskaran, Hui Qu, Yikai Zhang, Tong Zhang, Shaoting Zhang, and Dimitris N Metaxas. Multi-modal asyndgan: Learn from distributed medical image data without sharing private information. *arXiv preprint arXiv:2012.08604*, 2020.

Jieneng Chen, Yongyi Lu, Qihang Yu, Xiangde Luo, Ehsan Adeli, Yan Wang, Le Lu, Alan L Yuille, and Yuyin Zhou. Transunet: Transformers make strong encoders for medical image segmentation. *arXiv preprint arXiv:2102.04306*, 2021.

Reuben Dorent, Samuel Joutard, Marc Modat, Sébastien Ourselin, and Tom Vercauteren. Hetero-modal variational encoder-decoder for joint modality completion and segmentation. In *International Conference on Medical Image Computing and Computer-Assisted Intervention*, pages 74–82. Springer, 2019.

Alexey Dosovitskiy, Lucas Beyer, Alexander Kolesnikov, Dirk Weissenborn, Xiaohua Zhai, Thomas Unterthiner, Mostafa Dehghani, Matthias Minderer, Georg Heigold, Sylvain Gelly, et al. An image is worth 16x16 words: Transformers for image recognition at scale. *arXiv preprint arXiv:2010.11929*, 2020.

Mohammad Havaei, Nicolas Guizard, Nicolas Chapados, and Yoshua Bengio. Hemis: Hetero-modal image segmentation. In *International Conference on Medical Image Computing and Computer-Assisted Intervention*, pages 469–477. Springer, 2016.

Moein Heidari, Amirhossein Kazerouni, Milad Soltany, Reza Azad, Ehsan Khodapanah Aghdam, Julien Cohen-Adad, and Dorit Merhof. Hiformer: Hierarchical multi-scale representations using transformers for medical image segmentation. *arXiv preprint arXiv:2207.08518*, 2022.

Xiaohong Huang, Zhifang Deng, Dandan Li, and Xueguang Yuan. Missformer: An effective medical image segmentation transformer. *arXiv preprint arXiv:2109.07162*, 2021.

Kenneth Lau, Jonas Adler, and Jens Sjölund. A unified representation network for segmentation with missing modalities. *arXiv preprint arXiv:1908.06683*, 2019.

Ailiang Lin, Bingzhi Chen, Jiayu Xu, Zheng Zhang, Guangming Lu, and David Zhang. Ds-transunet: Dual swin transformer u-net for medical image segmentation. *IEEE Transactions on Instrumentation and Measurement*, 2022.

Han Liu, Yubo Fan, Hao Li, Jiacheng Wang, Dewei Hu, Can Cui, Ho Hin Lee, and Ipek Oguz. Moddrop++: A dynamic filter network with intra-subject co-training for multiple sclerosis lesion segmentation with missing modalities. *arXiv preprint arXiv:2203.04959*, 2022.

Bjoern H Menze, Andras Jakab, Stefan Bauer, Jayashree Kalpathy-Cramer, Keyvan Farahani, Justin Kirby, Yuliya Burren, Nicole Porz, Johannes Slotboom, Roland Wiest, et al. The multimodal brain tumor image segmentation benchmark (brats). *IEEE transactions on medical imaging*, 34(10):1993–2024, 2014.

Zhiwei Qin, Zhao Liu, Ping Zhu, and Wenyuan Ling. Style transfer in conditional gans for cross-modality synthesis of brain magnetic resonance images. *Computers in Biology and Medicine*, 148:105928, 2022.

Anil Rahate, Rahee Walambe, Sheela Ramanna, and Ketan Kotecha. Multimodal co-learning: challenges, applications with datasets, recent advances and future directions. *Information Fusion*, 81:203–239, 2022.

Olaf Ronneberger, Philipp Fischer, and Thomas Brox. U-net: Convolutional networks for biomedical image segmentation. In *International Conference on Medical image computing and computer-assisted intervention*, pages 234–241. Springer, 2015.

Ramprasaath R Selvaraju, Michael Cogswell, Abhishek Das, Ramakrishna Vedantam, Devi Parikh, and Dhruv Batra. Grad-cam: Visual explanations from deep networks via gradient-based localization. In *Proceedings of the IEEE international conference on computer vision*, pages 618–626, 2017.

Anmol Sharma and Ghassan Hamarneh. Missing mri pulse sequence synthesis using multi-modal generative adversarial network. *IEEE transactions on medical imaging*, 39(4): 1170–1183, 2019.

Zhuoran Shen, Mingyuan Zhang, Haiyu Zhao, Shuai Yi, and Hongsheng Li. Efficient attention: Attention with linear complexities. In *Proceedings of the IEEE/CVF winter conference on applications of computer vision*, pages 3531–3539, 2021.

Jeya Maria Jose Valanarasu, Vishwanath A Sindagi, Ilker Hacihaliloglu, and Vishal M Patel. Kiu-net: Towards accurate segmentation of biomedical images using over-complete representations. In *International conference on medical image computing and computer-assisted intervention*, pages 363–373. Springer, 2020.

Thomas Varsavsky, Zach Eaton-Rosen, Carole H Sudre, Parashkev Nachev, and M Jorge Cardoso. Pimms: permutation invariant multi-modal segmentation. In *Deep Learning in Medical Image Analysis and Multimodal Learning for Clinical Decision Support*, pages 201–209. Springer, 2018.

Yixin Wang, Yang Zhang, Yang Liu, Zihao Lin, Jiang Tian, Cheng Zhong, Zhongchao Shi, Jianping Fan, and Zhiqiang He. Acn: Adversarial co-training network for brain tumor segmentation with missing modalities. In *International Conference on Medical Image Computing and Computer-Assisted Intervention*, pages 410–420. Springer, 2021.

Hang Zhao, Orazio Gallo, Iuri Frosio, and Jan Kautz. Loss functions for image restoration with neural networks. *IEEE Transactions on computational imaging*, 3(1):47–57, 2016.

Zechen Zhao, Heran Yang, and Jian Sun. Modality-adaptive feature interaction for brain tumor segmentation with missing modalities. In *International Conference on Medical Image Computing and Computer-Assisted Intervention*, pages 183–192. Springer, 2022.

Zongwei Zhou, Md Mahfuzur Rahman Siddiquee, Nima Tajbakhsh, and Jianming Liang. Unet++: A nested u-net architecture for medical image segmentation. In *Deep learning in medical image analysis and multimodal learning for clinical decision support*, pages 3–11. Springer, 2018.

Appendix A. Details on Network Architecture

The MMCFormer framework employs a pure Transformer-based hierarchical U-Net structure that builds upon a 3D efficient Transformer. As shown in Figure 3(a), there are two paths incorporated in the proposed model, namely the full-modality and the missing-modality paths. Both paths use the same structure but with different input data. In each path, the input image $X \in R^{H \times W \times D \times C}$ is first processed by a patch embedding module, which creates overlapping patch tokens of size $4 \times 4 \times 4$. These tokens are then processed by the encoder, which consists of three stacked encoder blocks. Each block contains two successive 3D efficient Transformer layers and a patch merging layer that merges $2 \times 2 \times 2$ patch tokens to reduce the spatial dimension while doubling the channel dimension. This hierarchical representation enables the model to acquire an overview of multiple scales and enhance the feature representations. In the decoder, the patch-expanding block increases the number of tokens by a factor of 2. The output of each patch-expanding block is then fused with the features from the corresponding encoder layer using a linear layer to recover spatial and fine-grained information. The resulting features are subsequently passed into two 3D efficient Transformer layers. Finally, a linear projection layer generates the final segmentation map.

For the extra full-modality path, we define four modality-specific tokens entered into the bottleneck. We then design a modality reconstruction task to ensure that each token learns specific modality information. One of the four tokens is then randomly selected and fed into the single 3D efficient Transformer layer along with the resultant feature map obtained from the last skip connection in order to reconstruct the specific modality assigned to the token. A 3D upsampling module followed by a linear reconstruction head is finally applied to acquire the modality-specific reconstruction image.

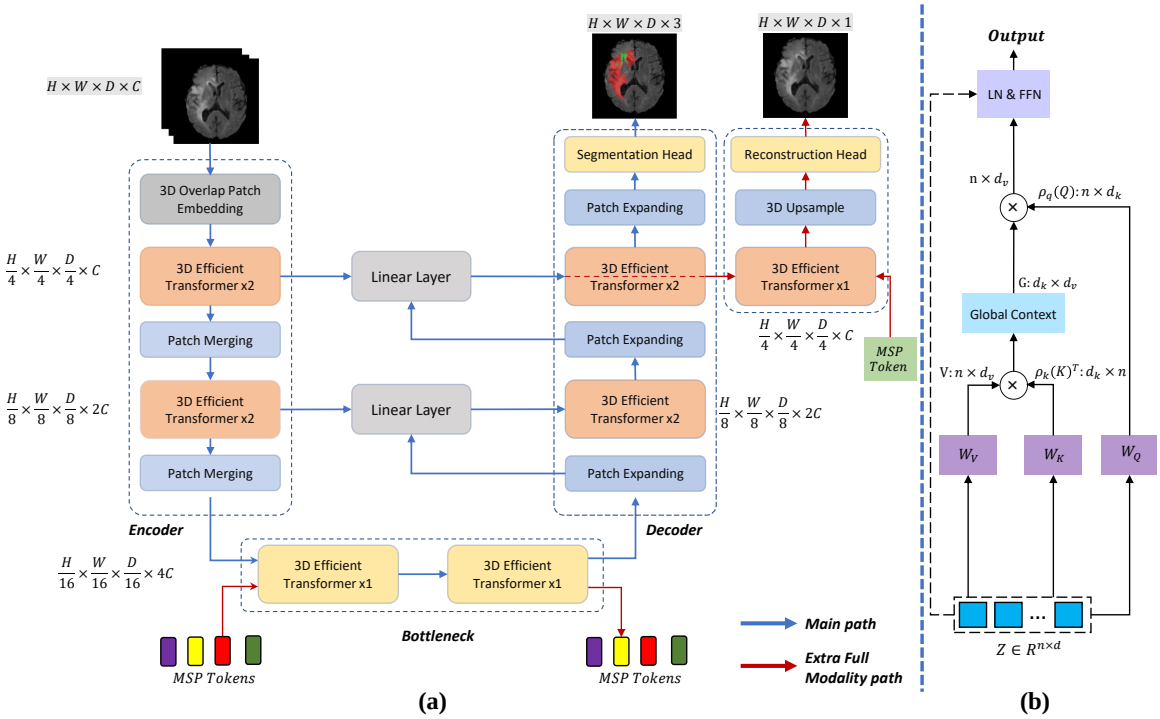

Figure 3: (a) The overview of the proposed network structure. (b) The structure of efficient Transformer.

Appendix B. Extreme Missing Modality

To further provide an insight into the effectiveness of our suggested framework for reconstructing the missing information, we offer quantitative and qualitative results in extremely missing modalities setting as presented in (Azad et al., 2022c). In this respect, we follow (Azad et al., 2022c) and design a scenario where during the training process the missing modality path only uses a single modality to learn the brain tumour segmentation map while benefiting from the full-modality path. During the test time, we only use the trained missing-modality path with a single modality as an input. Table 3 illustrates the quantitative results. For the comparison, we also include our baseline model, which consists of the co-trained Transformer-based U-Net model without any knowledge distillation mechanism. Quantitative results demonstrate that the MMCFormer surpasses the U-Net baseline method significantly. Besides that, our method achieves competitive results on all single modalities compared to the SOTA approaches. More specifically, in the T1ce and T2 modalities, our network surpasses the ACN and SMU-Net models by a large margin. Similarly, for the Flair modality, our method performs better compared to the ACN and HeMIS, HVED, and SMU-Net methods. In the T1 modality, we observed a large improvement compared to our baseline and approach but slightly less performance comparing to the ACN network. The obtained results prove the efficacy of the suggested framework in learning task-specific patterns and recovering the missing information.

To visually analyze the qualitative performance of our suggested framework, we have provided the Grad-CAM (Selvaraju et al., 2017) attention maps in Figure 4-Figure 7 for each

Table 3: Quantitative results of the proposed MMCFormer model against the SOTA approaches on BraTS 2018 series with extreme missing modality scenario. We use the average of the whole, enhanced and core tumour segmentation scores to report the dice score for each modality.

Article	**Dice score**				
	T1	**T1c**	**T2**	**FLAIR**	**AVG**
Our Baseline	61.2	77.3	60.1	58.2	64.2
U-HeMIS (Havaei et al., 2016)	16.7	59.2	36.0	51.5	48.8
HVED (Dorent et al., 2019)	34.4	64.8	55.2	52.4	51.7
ACN (Wang et al., 2021)	**63.8**	80.3	64.6	65.3	68.5
SMU-net (Azad et al., 2022c)	63.3	80.9	65.3	68.4	69.4
MMCFormer	63.6	**82.0**	**68.2**	**68.6**	**70.6**

modality. In this respect, we trained and evaluated the network with an extremely missing modality setting. It can be seen that the MMCFormer localizes the brain tumour region with high confidence in a single modality case. This illustrates the effect of our co-training strategy for recovering the missing information. Additionally, the T1 modality is more effective for characterizing the structural information and less informative for detecting for core tumour region, however, our MMCFormer with a T1 modality can recognize the tumour region with high confidence which indicates the importance of our suggested modules for recovering the missing information. Similarly for other modalities, we can observe that the activation map has a high magnitude around the tumour region and it highly overlaps with the grand truth annotation mask. On top of that, we can observe that the MMCFormer attention has less variance and it is in line with the ground truth map, which shows the effect of reconstructed features for precise boundary prediction.

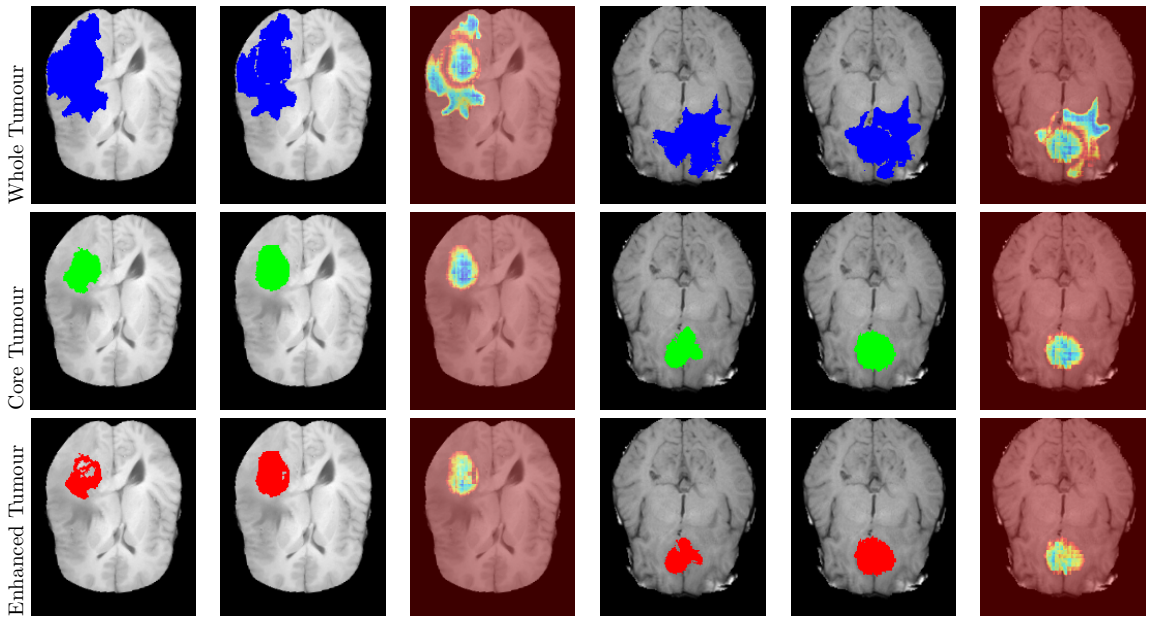

(a) Ground Truth (b) Prediction (c) Heatmap (d) Ground Truth (e) Prediction (f) Heatmap

Figure 4: Visualization of the activation map on T1 modality using our suggested MMCFormer.

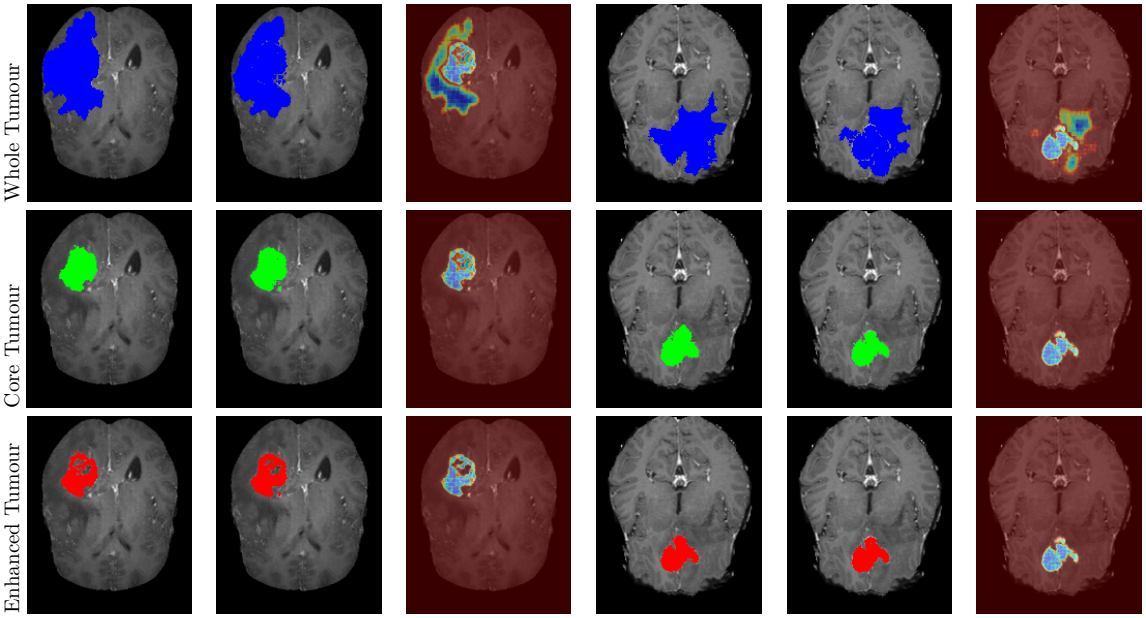

(a) Ground Truth (b) Prediction (c) Heatmap (d) Ground Truth (e) Prediction (f) Heatmap

Figure 5: Visualization of the activation map on T1c modality using our suggested MMCFormer.

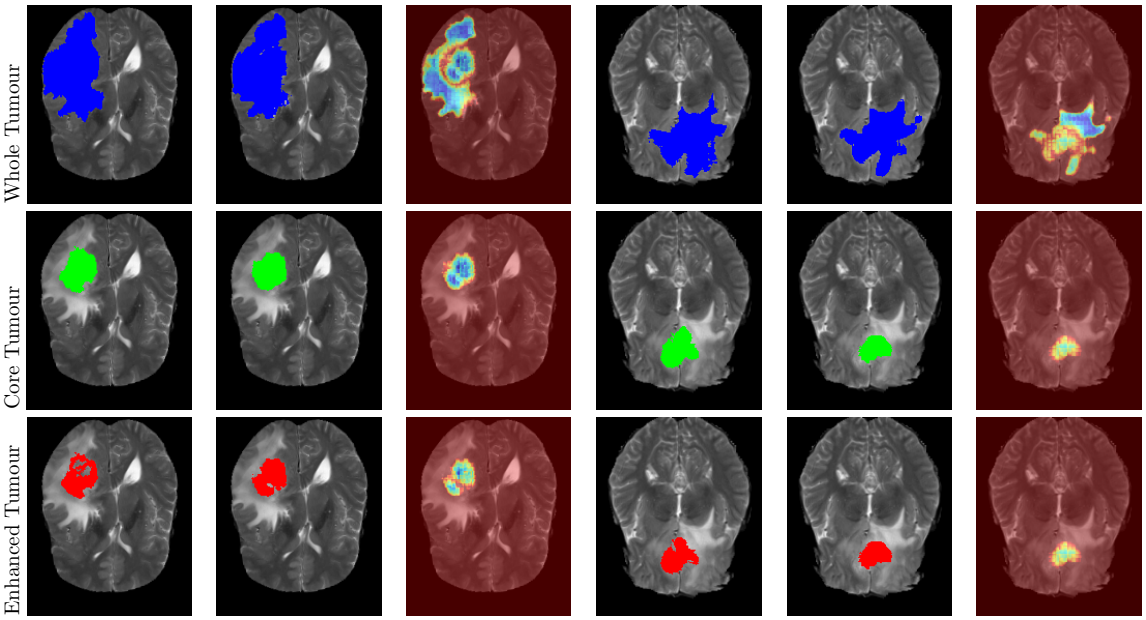

(a) Ground Truth (b) Prediction (c) Heatmap (d) Ground Truth (e) Prediction (f) Heatmap

Figure 6: Visualization of the activation map on T2 modality using our suggested MMCFormer.

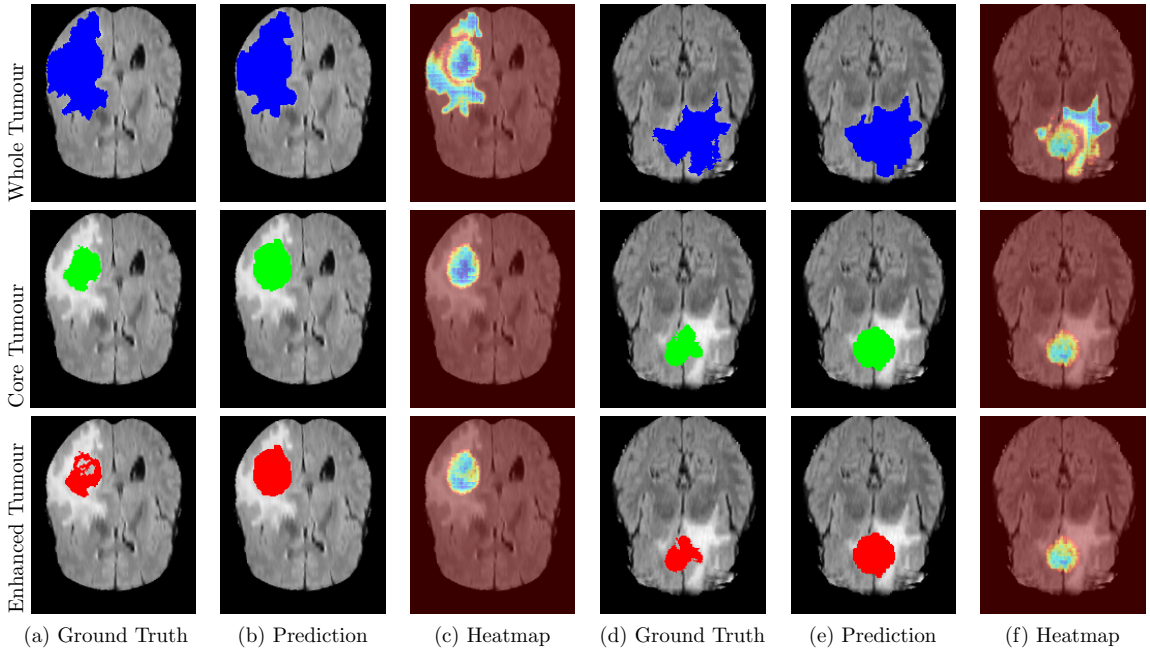

Figure 7: Visualization of the activation map on Flair modality using our suggested MMCFormer.

Appendix C. Reconstruction Head

In our strategy, we included the reconstruction head to reconstruct each MRI modality during the training time. The objective of the reconstruction head in our design is to guide the network through the learning modality-specific feature and transfer such discriminative information to the missing modality network. To ensure the performance of our reconstruction head as an auxiliary task, we visualize the reconstructed modality in Figure 8 along with the error map. We use a pixel-wise difference for calculating the error mask. It can be seen that for all modalities, our network manages to reconstruct the images with good quality and an acceptable error rate. There is also a high potential for more fine-grained reconstruction by increasing the complexity of the reconstruction head, however, the reconstruction is not the main task in our design and therefore we use a simple reconstruction head to fulfill the objective. It is also worthwhile to mention that in our strategy we utilize the combination of MS-SSIM and L1 distances for the reconstruction loss. Although including the MS-SSIM loss enhances the reconstruction loss, it requires more computation complexity. Hence, one might consider such complexity in their use case.

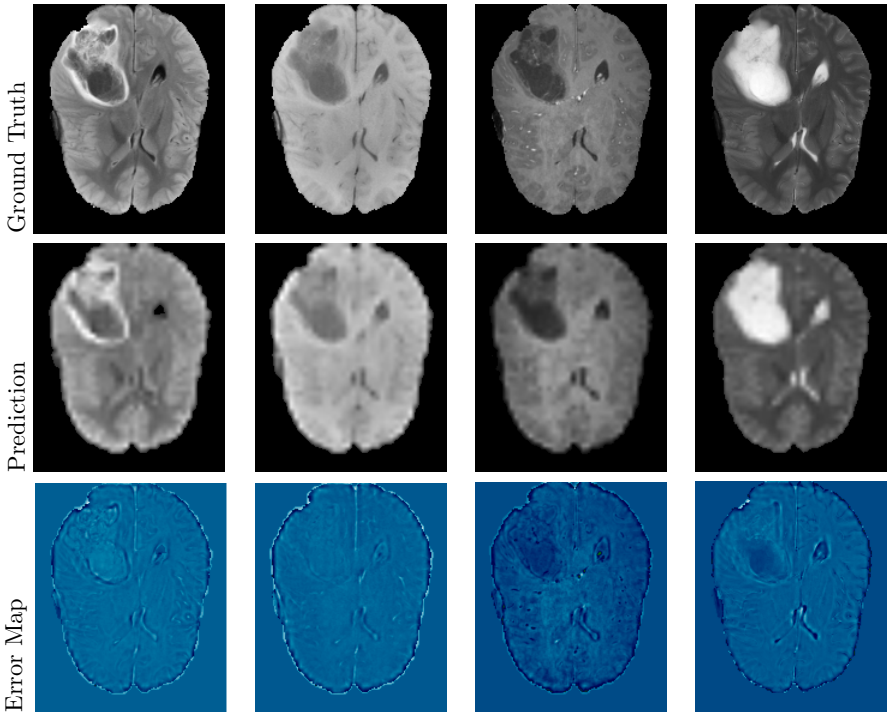

(a) Flair (b) T1 (c) T1c (d) T2

Figure 8: Visual reconstruction of Flair, T1, T1c, and T2 modalities, along with the error map between the reconstructed results and the ground truth.